

LETTER TO THE EDITOR

# Turbulent and fast motions of H<sub>2</sub> gas in active galactic nuclei

K. M. Dasyra<sup>1,2</sup> and F. Combes<sup>2</sup>

<sup>1</sup> Laboratoire AIM, CEA/DSM-CNRS-Université Paris Diderot, Irfu/Service d'Astrophysique, CEA Saclay, F-91191 Gif-sur-Yvette, France

<sup>2</sup> Observatoire de Paris, LERMA (CNRS:UMR8112), 61 Av. de l'Observatoire, F-75014, Paris, France

## ABSTRACT

Querying the *Spitzer* archive for optically-selected active galactic nuclei (AGN) observed in high-resolution-mode spectroscopy, we identified radio and/or interacting galaxies with highly turbulent motions of H<sub>2</sub> gas at a temperature of a few hundred Kelvin. Unlike all other AGN that have unresolved H<sub>2</sub> line profiles at a spectral resolution of  $\sim 600$ , 3C236, 3C293, IRAS09039+0503, MCG-2-58-22 and Mrk463E have intrinsic velocity dispersions exceeding  $200 \text{ km s}^{-1}$  for at least two of the rotational S0, S1, S2, and S3 lines. In a sixth source, 4C12.50, a blue wing was detected in the S1 and S2 line profiles, indicating the presence of a warm molecular gas component moving at  $-640 \text{ km s}^{-1}$  with respect to the bulk of the gas at systemic velocity. Its mass is  $5.2 \times 10^7 M_{\odot}$ , accounting for more than one fourth of the H<sub>2</sub> gas at 374K, but less than 1% of the cold H<sub>2</sub> gas computed from CO observations. Because no diffuse gas component of 4C12.50 has been observed to date to be moving at more than  $250 \text{ km s}^{-1}$  from systemic velocity, the H<sub>2</sub> line wings are unlikely to be tracing gas in shock regions along the tidal tails of this merging system. They can instead be tracing gas driven by a jet or entrained by a nuclear outflow, which is known to emerge from the west nucleus of 4C12.50. It is improbable that such an outflow, with an estimated mass loss rate of  $130 M_{\odot} \text{ yr}^{-1}$ , entirely quenches the star formation around this nucleus.

**Key words.** ISM: jets and outflows — ISM: kinematics and dynamics — Line: profiles — Galaxies: active — Galaxies: nuclei — Infrared: galaxies

## 1. Introduction

Large-scale feedback effects such as jets and outflows from active galactic nuclei (AGN) are thought to be capable of affecting the formation of new stars in their host galaxies. The triggering of star formation by compression of gas (e.g., van Breugel et al., 1985), as well as the suppression of star formation by heating of gas that prevents its further collapse (e.g., Nesvadba et al., 2010) have been observed in local AGN. Cosmological simulations have suggested that AGN feedback effects, which are often associated with mergers, could make galaxies appear red, or even explain the observed luminosity functions of galaxies (Croton et al., 2006; Hopkins et al., 2006). Combined with multi-wavelength observations indicating that the star-formation history and the black-hole-accretion history of the Universe peak at comparable redshifts, between  $1 \lesssim z \lesssim 3$  (Marconi et al., 2004; Merloni et al., 2004), this suggests that AGN feedback could have affected the shape of present-day galaxies considerably.

Extensive tests of the role of AGN feedback on the interstellar medium (ISM) of galaxies require a detailed kinematic study of outflowing gas in local sources. Signs of massive gas outflows have been detected for ionized atomic gas (e.g., Veilleux et al., 1995; Emonts et al., 2005; Holt et al., 2006; Müller-Sánchez et al., 2006), neutral atomic gas (e.g., Morganti et al., 2005; Rupke et al., 2005), and molecular CO and OH gas (e.g., Curran et al., 1999; Das et al., 2005; García-Burillo et al., 2009; Sakamoto et al., 2009; Feruglio

et al., 2010; Fischer et al., 2010; Sturm et al., 2011). In this letter we present evidence for the first detection of highly turbulent motions of H<sub>2</sub> gas at a temperature of a few hundred Kelvin as seen with *Spitzer* for several local AGN. We adopt  $H_0=70 \text{ km s}^{-1} \text{ Mpc}^{-1}$ ,  $\Omega_M=0.3$ , and  $\Omega_{\Lambda}=0.7$  throughout this work.

## 2. The sample selection

We queried for turbulence in the warm H<sub>2</sub> gas in local AGN using mid-IR spectra obtained with *Spitzer* in high-resolution mode. The full archival sample comprises 298 sources that are classified as AGN based on optical spectroscopy. It is presented in Dasyra et al. (2011) together with the data reduction techniques and the extracted spectra.

To look for turbulent H<sub>2</sub> gas motions, we examined the profiles of the purely rotational (0-0)S0 28.22  $\mu\text{m}$ , (0-0)S1 17.04  $\mu\text{m}$ , (0-0)S2 12.28  $\mu\text{m}$ , and (0-0)S3 9.66  $\mu\text{m}$  lines. We searched for either resolved profiles with velocity dispersion  $\sigma \gtrsim 200 \text{ km s}^{-1}$ , or for profiles with asymmetric wings that are characteristic of outflows. To ensure the reliability of our results, we only examined sources with at least two lines of signal-to-noise (S/N) ratio  $>5$ . We also requested that at least two lines suggest a similar kinematic pattern, i.e. a wing or a resolved profile. To consider a line resolved we requested that its full width at half maximum (FWHM) value minus the FWHM error exceeds the instrumental resolution  $R$  plus the resolution error at the observed-frame

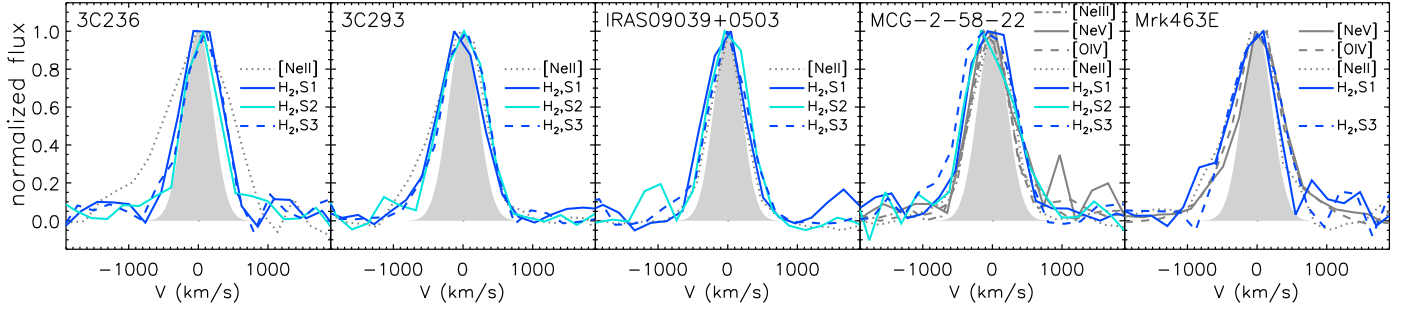


**Fig. 1.** Normalized, continuum-subtracted molecular and ionized gas line profiles in local AGN with resolved H<sub>2</sub> emission. The filled gray area represents a Gaussian with FWHM equal to the resolution of the IRS.

**Table 1.** Fluxes and widths of resolved H<sub>2</sub> lines in local AGN.

Source	$z$	$f_{S1}$ $10^{-17} \text{ W m}^{-2}$	$\text{FWHM}_{S1}^a$ $\text{km s}^{-1}$	$f_{S2}$ $10^{-17} \text{ W m}^{-2}$	$\text{FWHM}_{S2}^a$ $\text{km s}^{-1}$	$f_{S3}$ $10^{-17} \text{ W m}^{-2}$	$\text{FWHM}_{S3}^a$ $\text{km s}^{-1}$	$M_{warm}$ $10^7 M_{\odot}$	T K	$M_{cold}^b$ $10^9 M_{\odot}$
3C236	0.0989	$1.06 \pm 0.07$	582 (750)	$0.49 \pm 0.08$	557 (719)	$0.81 \pm 0.09$	624 (767)	6.10	345	<5.1
3C293	0.0450	$5.30 \pm 0.38$	510 (716)	$1.79 \pm 0.31$	553 (732)	$2.96 \pm 0.38$	519 (714)	6.62	323	23
IRAS09039+0503	0.1254	$3.09 \pm 0.54$	519 (700)	$1.34 \pm 0.06$	575 (730)	$2.04 \pm 0.13$	569 (751)	31.6	334	...
MCG-2-58-22	0.0472	$3.86 \pm 0.42$	544 (740)	$1.50 \pm 0.25$	636 (796)	$3.40 \pm 0.46$	662 (824)	4.19	359	5.7
Mrk463E	0.0507	$3.37 \pm 0.59$	556 (748)	<1.98	...	$3.76 \pm 0.44$	590 (767)	4.06	378	1.2
4C12.50 (main <sup>c</sup> )	0.1217	$1.64 \pm 0.21$	... (519)	$1.20 \pm 0.11$	... (552)	$1.78 \pm 0.46$	... (652)	13.9	374	15
4C12.50 (wing <sup>e</sup> )	0.1196 <sup>d</sup>	$0.62 \pm 0.21$	... (568)	$0.44 \pm 0.11$	521 (690)	...	... (...)	5.19	374 <sup>e</sup>	...

**Notes.** None of these sources had a reliable S0 detection owing to the high noise levels in the long wavelength array. <sup>(a)</sup> Rest-frame, instrumental-broadening-corrected FWHM. Their measured values appear in parenthesis. Their error bars correspond to 5–10% of their values. <sup>(b)</sup> Cold H<sub>2</sub> gas masses calculated from CO observations (Evans et al., 1999, 2002; Bertram et al., 2007; Saripalli & Mack, 2007) using an H<sub>2</sub>/CO mass conversion factor of  $1.5 M_{\odot}/(\text{K km s}^{-1} \text{pc}^2)$  for the IR-bright systems Mrk463E and 4C12.50 (Evans et al., 2002), and a standard Galactic value of  $4.8 M_{\odot}/(\text{K km s}^{-1} \text{pc}^2)$  for all other sources. They are converted to the adopted cosmology. <sup>(c)</sup> The main and wing components correspond to the primary and the secondary Gaussian functions in Figure 2. <sup>(d)</sup> The Gaussians that best fit the S1 and S2 line wings peak at  $-646 \text{ km s}^{-1}$  and  $-634 \text{ km s}^{-1}$  from systemic velocity, respectively. <sup>(e)</sup> The excitation temperature of the rapidly moving H<sub>2</sub> gas is assumed to be identical to that of the H<sub>2</sub> at systemic velocity to facilitate the comparison of their masses.

wavelength of the line (Dasyra et al., 2011). The average  $R$  value in the  $12.0\text{--}18.0 \mu\text{m}$  range, which comprises the H<sub>2</sub> S1 and S2 transitions, is  $507 \pm 66 \text{ km s}^{-1}$ .

### 3. Results: Sources with highly turbulent or rapidly moving H<sub>2</sub> gas in the warm phase

Of the 298 sources 62 had at least two H<sub>2</sub> lines detected with  $S/N > 5$ . The profiles of two or more lines were spectrally resolved in only five sources, namely 3C236, 3C293, IRAS09039+0503, MCG-2-58-22, and Mrk463E (Fig. 1). Their velocity dispersions are in the range  $220 \lesssim \sigma \lesssim 280 \text{ km s}^{-1}$  (Table 1). Because all these sources are radio galaxies and/or interacting systems, the high turbulence in their warm H<sub>2</sub> motions can be driven by AGN feedback mechanisms, by gravitational instabilities, or by supernova winds. Still, no mechanism is efficient enough to kinematically distort a detectable mass of warm H<sub>2</sub> gas to velocity dispersions exceeding  $300 \text{ km s}^{-1}$ . We computed the excitation temperature  $T$  and mass of the turbulent gas (Table 1) using the detected S1, S2, and S3 line fluxes as in Higdon et al. (2006). At temperatures of  $300\text{--}400 \text{ K}$ , its mass is typically on the order of 1% of the cold H<sub>2</sub> gas mass indicated by CO observations.

Further outflow or inflow signatures were sought for in the H<sub>2</sub> line wings and in the difference of the H<sub>2</sub> recession velocity from the systemic velocity,  $V_{sys}$ . The latter was determined from the [Ne II] line, emitted by

ions that are abundant in star-forming regions and in the AGN vicinity owing to their low ionization potential, 21.56 eV. The H<sub>2</sub> recession velocity agreed within the errors with  $V_{sys}$  for all sources, including those with massive outflows of the gas that is photoionized by the AGN and that is traced by the [Ne V] or [O IV] lines (i.e., 3C273, IRAS13342+3932, IRAS05189-2524, IRAS15001+1433, IRAS23060+0505, Mrk609; Dasyra et al., 2011).

The only source with wing signatures in its H<sub>2</sub> line profiles was 4C12.50, also known as IRAS13451+1232 or PKS1341+12. The S1 and S2 line wings (Fig. 2; upper panel), detected with  $S/N \gtrsim 3$ , point at two warm molecular gas kinematic components in this source. The peak of the secondary Gaussian that is needed to fit both profiles is blueshifted by  $\sim 640 \text{ km s}^{-1}$  from the primary Gaussian at  $V_{sys}$ . The flux ascribed to the primary Gaussian is only 2.6 and 2.7 times higher than that ascribed to the secondary Gaussian of the S1 and S2 transitions, respectively. Using the actual flux in each Gaussian (Table 1), we separately calculated the H<sub>2</sub> gas mass for each kinematic component. We find the excitation temperature of the bulk of the gas to be  $374 \pm 12 \text{ K}$ . It is equal to the inverse of the slope of the line that best fits the excitation diagram points (Rigopoulou et al., 2002). The excitation diagram (Fig. 2; lower panel) shows the natural logarithm of the number of electrons  $n_e$  that descended from the upper to the lower state, normalized by the statistical weight  $g$  of the transi-

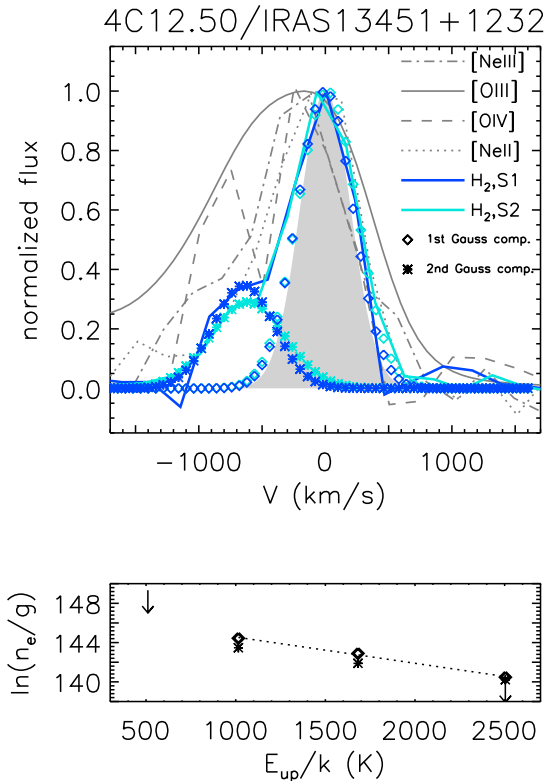


**Fig. 2.** Upper panel: Normalized, continuum-subtracted molecular and ionized gas line profiles for 4C12.50. In addition to the profiles of the MIR lines, the 5007 Å [O III] profile that is convolved to the resolution of IRS is presented for comparison. The blue wing is detected in all lines except for the unresolved S3. Lower panel: H<sub>2</sub> excitation diagram constructed separately for the primary Gaussian component (open diamonds) and the secondary Gaussian component (stars) of each H<sub>2</sub> line.

tion, as a function of the temperature that corresponds to the energy of the upper state  $E_{up}$  divided by the Boltzmann constant  $k$ . The value of  $n_e$  is computed as  $L/(\alpha h\nu)$ , where  $h$  is the Planck constant,  $\alpha$  is the Einstein coefficient of the transition, and  $\nu$  is the frequency of the emitted line. For a single temperature of 374K we find that the mass of the H<sub>2</sub> gas at systemic velocity is  $1.4 \times 10^8 M_\odot$  (see also Higdon et al., 2006). Assuming (for simplicity) that  $T$  is the same for both H<sub>2</sub> kinematic components (see Figure 2), we find that the mass of the H<sub>2</sub> gas moving at  $640 \text{ km s}^{-1}$  is  $5.2 \times 10^7 M_\odot$ . This is 0.3% of the cold H<sub>2</sub> gas mass in the west nucleus of 4C12.50, which was found from CO observations to be  $1.5 \times 10^{10} M_\odot$  (Evans et al., 2002).

#### 4. Discussion: An AGN-driven molecular gas outflow in 4C12.50?

Even though 4C12.50 is an IR-bright system of two interacting galaxies (Axon et al., 2000), the secondary Gaussian of Figure 2 is unlikely to be tracing gas in the east nucleus, which is mostly located outside the IRS slit (Fig. 3). Any residual gas from the east nucleus inside the slit would be moving at a velocity comparable to the difference in the recession velocity of the two nuclei,  $\sim 200 \text{ km s}^{-1}$ . This difference is computed from ionized gas kinematics (Holt et al., 2003), and it is confirmed by stellar kinematics from CO absorption features presented in Dasyra et al. (2006).

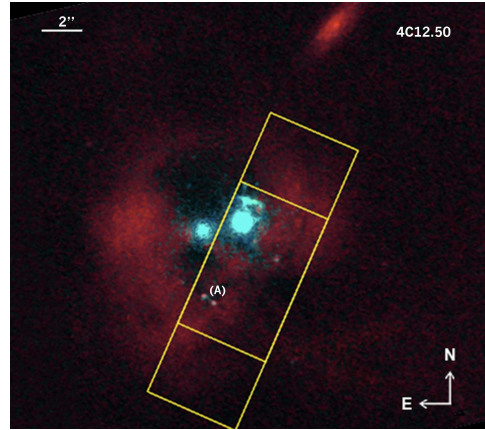


**Fig. 3.** Composite H $\alpha$  (cyan) and 5900 Å continuum (red) image of 4C12.50, constructed from *Hubble* Space Telescope data (Batcheldor et al., 2007). To enhance the visibility of low surface brightness structures, we removed all symmetric galaxy components (i.e., a common bulge and two residual disks located at the position of the two nuclei) from the 5900 Å image with GALFIT (Peng et al., 2002). Both disks were found to have an inclination of  $\sim 20^\circ$ . Irregularly moving components are found within the IRS slit, marked with a yellow box for both nod positions. (A) marks the position of two super star clusters with velocities that are blueshifted by up to  $\sim 250 \text{ km s}^{-1}$  from systemic velocity (Rodríguez Zaurín et al., 2007).

Besides the two nuclei residing in a common bulge, 4C12.50 also has off-nuclear gas concentrations and super star clusters in tidal tails. The blueshifted H<sub>2</sub> emission could arise from gas in a tidal tail inside the IRS slit (Fig. 3), which is entering a shock front created during the collision (see Cluver et al., 2010). The tidal tail could be moving faster or be at a different inclination angle  $i$  than its corresponding nucleus, of  $\sim 20^\circ$  in either case. Because the deprojected tail velocity would be equal to  $640/\sin(i) \text{ km s}^{-1}$ , it could reach a value as high as  $\sim 2000 \text{ km s}^{-1}$ . This scenario is also unlikely given that no off-nuclear, large-scale ( $< 20 \text{ kpc}$ ) kinematic component has been observed to be moving faster than  $\pm 250 \text{ km s}^{-1}$  from  $V_{sys}$  along the line of sight (Holt et al., 2003; Rodríguez Zaurín et al., 2007).

A scenario that agrees better with existing observations is that the H<sub>2</sub> gas is moving toward us driven by feedback mechanisms (e.g., Alatalo et al., 2011). Optical spectroscopy indicated the presence of an outflow from the west nucleus of 4C12.50 by revealing the existence of three kinematic components for the nuclear [O I], [S II], and [O III] emission (Holt et al., 2003). Most of the [O III] emission is blueshifted by  $400 \text{ km s}^{-1}$ , while its broadest component (of FWHM  $\sim 1900 \text{ km s}^{-1}$ ) is blueshifted by  $2000 \text{ km s}^{-1}$  from  $V_{sys}$ . MIR spectroscopy suggested an AGN-related nuclear outflow of ionized gas. Blue wings were observed in the profiles of the [O IV]  $25.89 \mu\text{m}$  and the [Ne V]  $14.32 \mu\text{m}$  lines (Spoon & Holt, 2009; Dasyra et al., 2011), emitted by ions that are primarily found in hard radiation fields. Radio observations revealed an HI absorption line blueshifted by  $\sim 1000 \text{ km s}^{-1}$  from  $V_{sys}$  (Morganti et al., 2004). Because a background radio source is required for HI absorption to be seen, the hydrogen clouds are likely to be located between the observer and the AGN or its jet. Estimates of the outflow mass range from  $8 \times 10^5 M_\odot$  for the ionized  $10^4 \text{ K}$  gas (Holt et al., 2011) to  $5.6 \times 10^8 M_\odot$  for the neu-

tral gas traced by NaID (Rupke et al., 2005), bracketing our mass estimate,  $M_{out}$ , of  $5.2 \times 10^7 M_{\odot}$  for the outflowing  $\sim 400\text{K}$  H<sub>2</sub> gas.

If the outflow is caused by AGN radiation pressure or winds (Holt et al., 2011), it can be considered spherical. If the gas is also distributed in a sphere, and if its density is falling with the inverse square of the distance from the center, its mass outflow rate,  $\dot{M}$ , will be given from the product  $M_{out}V_{out}R^{-1}$ . For an outflow velocity  $V_{out}$  of  $640\text{ km s}^{-1}$  and for a radius  $R$  of 270 pc, as estimated for the CO gas assuming that it is thermalized to the dust temperature (Evans et al., 2002) and as converted to the adopted cosmological distance,  $\dot{M}$  will be  $130 M_{\odot}\text{ yr}^{-1}$ . An outflow of these properties is unlikely to entirely suppress star formation in the west nucleus of 4C12.50, whose star-formation rate (SFR) is estimated to be between 370–1380  $M_{\odot}\text{ yr}^{-1}$ . The lower value is found from the CO mass using a gas consumption timescale of  $4 \times 10^7$  yrs, while the upper value is found by folding the CO-based H<sub>2</sub> mass and radial extent in the Schmidt-Kennicutt law (Evans et al., 2002). If the outflow were symmetric, both a blue and a red H<sub>2</sub> line profile wing should exist unless the gas moving away from the observer is obscured by dust. This is plausible for a source with E(B-V) of 1.44 magnitudes (Holt et al., 2011) and  $9.7\text{ }\mu\text{m}$  optical depth of 0.59 (Veilleux et al., 2009), which could translate into a 10–20% absorption of the total flux at  $17\text{ }\mu\text{m}$  (Li & Draine, 2001), and which could preferentially suppress the red line wing for a circumnuclear dust distribution.

Alternatively, a radio jet encountering clouds on its path could be driving the outflow (e.g., Dietrich & Wagner, 1998). A jet is indeed known to emerge from the west nucleus of 4C12.50. It extends out to 45 pc in projection in the north and 170 pc in the south (Stanghellini et al., 1997), and it propagates close to the speed of light at a small angle from the line of sight (Lister et al., 2003). A previous flare of the jet, undetected in the radio because of its weak signal, could be associated with the shocked gas whose extended X-ray emission peaks at 20 kpc south of the nucleus (Siemiginowska et al., 2008). The scenario of a jet-driven outflow can easily explain the observed line profiles. The detection of a blue or a red wing is random since it depends on the location of the clouds with respect to the jet propagation axis.

## 5. Summary and concluding remarks

We queried the archival catalog of 298 optically-selected AGN observed with *Spitzer* IRS in high-resolution mode (Dasyra et al., 2011), aiming to identify sources with turbulent motions of their warm molecular gas. We examined the profiles of the H<sub>2</sub> S0, S1, S2, and S3 lines and found only five radio and/or interacting galaxies with  $\sigma > 200\text{ km s}^{-1}$  but no source with  $\sigma > 300\text{ km s}^{-1}$ . In a sixth source, 4C12.50, the S1 and S2 lines have a blue wing that points at warm gas moving toward us with  $640\text{ km s}^{-1}$ . Its mass,  $5.2 \times 10^7 M_{\odot}$ , corresponds to an impressively high fraction,  $\sim 1/4$ , of the total  $\sim 400\text{K}$  H<sub>2</sub> gas mass. While it could be tracing shock regions along tidal tails, it is more likely to be tracing an AGN jet or wind-driven outflow, known from ionized and neutral gas kinematic studies. Even if all of this gas is entrained by an outflow, it is unlikely to entirely suppress star formation in 4C12.50. Additional tests of the

role of AGN feedback mechanisms in increasing the turbulence of the molecular gas require observations of high-rotational-number transitions of CO molecules that can be mostly excited by the AGN (van der Werf et al., 2010). An essential role in revisiting this question will also be played by the Atacama Large Millimeter Array, which, via high-resolution studies of the cold gas, will enable a comparison never performed before: the computation of the warm-to-cold molecular gas mass ratio in an outflow vs the rest of the ISM.

*Acknowledgements.* K. D. acknowledges support by the European Community through a Marie Curie Fellowship (PIEF-GA-2009-235038) awarded under the 7th Framework Programme (2007-2013).

## References

- Alatalo, K., Blitz, L., Young, L. M., et al. 2011, *ApJ*, 735, 88  
 Axon, D. J., Capetti, A., Fanti, R., et al. 2000, *AJ*, 120, 2284  
 Batchelder, D., Tadhunter, C., Holt, J., et al. 2007, *ApJ*, 661, 70  
 Bertram, T., Eckart, A., Fischer, S., et al. 2007, *A&A*, 470, 571  
 Cluver, M. E., Appleton, P., Boulanger, F., et al. 2010, *ApJ*, 710, 248  
 Croton, D. J., Springel, V., White, S. D. M., et al., 2006, *MNRAS*, 367, 864  
 Curran, S. J., Rydbeck, G., Johansson, L. E. B., & Booth, R. S. 1999, *A&A*, 344, 767  
 Das, M., Vogel, S. N., Verdoes K. G. A., et al. 2005, *ApJ*, 629, 757  
 Dasyra, K. M., Tacconi, L. J., Davies, R. I., et al. 2006, *ApJ*, 638, 745  
 Dasyra, K. M., Ho, L. C., Netzer, H., et al. 2011, *ApJ*, in press, arXiv/1107.3397  
 Dietrich, M., & Wagner, S. J. 1998, *A&A*, 338, 405  
 Emonts, B. H. C., Morganti, R., Tadhunter, C. N., et al. 2005, *MNRAS*, 362, 931  
 Evans, A. S., Sanders, D. B., Surace, J. A., & Mazzarella, J. M. 1999 *ApJ*, 511, 730  
 Evans, A. S., Mazzarella, J. M., Surace, J. A., & Sanders, D. B. 2002 *ApJ*, 580, 749  
 Feruglio, C., Maiolino, R., Piconcelli, E., et al. 2010, *A&A*, 518, L155  
 Fischer, J., Sturm, E., González-Alfonso, E., et al. 2010, *A&A*, 518, L41  
 García-Burillo, S., Combes, F., Usero, A., & Fuente, A. 2009, *AN*, 330, 245  
 Higdon, S. J. U., Armus, L., Higdon, J. L., Soifer, B. T., & Spoon, H. W. W. 2006 *ApJ*, 648, 323  
 Holt, J., Tadhunter, C. N., & Morganti, R. 2003, *MNRAS*, 342, 227  
 Holt, J., Tadhunter, C. N., & Morganti, R. 2006, *AN*, 327, 147  
 Holt, J., Tadhunter, C. N., Morganti, R., & Emonts, B. H. C. 2011, *MNRAS*, 410, 1527  
 Hopkins, P. F., Somerville, R. S., Hernquist, L., et al. 2006, *ApJ*, 652, 864  
 Li, A. & Draine, B. T. 2001, *ApJ*, 554, 778  
 Lister, M. L., Kellermann, K. I., Vermeulen, R. C., et al. 2003, *ApJ*, L584, 135  
 Marconi, A., Risaliti, G., Gilli, R., et al. 2004, *MNRAS*, 351, 169  
 Merloni, A., Rudnick, G., & Di Matteo, T. 2004, *MNRAS*, 354, L37  
 Morganti, R., Oosterloo, T. A., Tadhunter, C. N., et al. 2004, *A&A*, 424, 119  
 Morganti, R., Tadhunter, C. N., & Oosterloo, T. 2005, *A&A*, 444, L9  
 Müller-Sánchez, F., Davies, R. I., Eisenhauer, F., et al. 2006, *A&A*, 454, 481  
 Nesvadba, N., Boulanger, F., Salomé, P., et al. 2010, *A&A*, 521, 65  
 Peng, C. Y., Ho, L. C., Impey, C., & Rix, H.-W. 2002, *AJ*, 124, 266  
 Rodríguez Zaurín, J., Holt, J., Tadhunter, C. N., & González Delgado, R. M. 2007, *MNRAS*, 375, 1133  
 Rigopoulou, D., Kunze, D., Lutz, D., et al. 2002 *A&A*, 389, 374  
 Rupke, D. S., Veilleux, S., & Sanders, D. B. 2005, *ApJ*, 632, 751  
 Sakamoto, K., Aalto, S., Wilner, D. J., et al. 2009, *ApJ*, L700, 104  
 Saripalli, L., & Mack, K.-H., *MNRAS*, 376, 1385  
 Siemiginowska, A., LaMassa, S., Aldcroft, T. L., et al. 2008, *ApJ*, 684, 811  
 Spoon, H. W. W., & Holt, J. 2009, *ApJ*, 702, L42  
 Stanghellini, C., O’Dea, C. P., Baum, S. A., et al. 1997 *A&A*, 325, 943  
 Sturm, E., González-Alfonso, E., Veilleux, S., et al. 2011, *ApJ*, 733, L16

- van Breugel, W., Filippenko, A. V., Heckman, T., & Miley, G. 1985, ApJ, 293, 83
- van der Werf, P. P., Isaak, K. G., Meijerink, R., et al. 2010, A&A, L518, 42
- Veilleux, S., Kim, D.-C., Sanders, D. B., et al. 1995, ApJS, 98, 171
- Veilleux, S., Rupke, D. S. N., Kim, D.-C., et al. 2009, ApJS, 182, 628